Pergamon

PII: S0191-8141(97)00092-8

Journal of Structural Geology, Vol. 20, No. 4, pp. 321 to 338, 1998

0191-8141/98 $19.00 + 0.00

The shaping of salt diapirs

HEMIN KOYI

Hans Ramberg Tectonic Laboratory (HRTL), Institute of Earth Sciences, Norbyvagen 18B, S-752 36 Uppsala, Sweden

(*Received* 27 *March* 1996; *accepted in revised form* 30 *September* 1997)

Abstract—Six parameters shape the geometry of passive diapirs associated with stiff overburden: rates of salt supply (S'); dissolution (D'); sediment accumulation (A'); erosion (Er'); extension (E'); and shortening (Sh'). These parameters change in space and time, and hence influence the geometry of the structure as it forms.

A complex six-parameter plot, representing the evolution history of a salt diapir, can be simplified into three separate graphs. This study recommends adding to plots of S' against A', a second of rate of salt supply (S'), this time with extension rate (E'), and a third of rate of sediment accumulation (A') plotted against extension rate (E'). Integrating these three plots on a single diagram results in a complete description of the evolution history of a diapir when it is applied to three-dimensional data. However, if applied to a profile, the plot shows only the two-dimensional evolution history of the diapir.

Lateral forces (extension or compression) have a significant role in moulding the geometry of a salt diapir by influencing the space which it occupies. By incorporating extension in the moulding plots of salt diapirs, this study introduces the rate of sediment accumulation multiplied by extension ($(E{\cdot}A)'$) as a significant factor in moulding salt diapirs. By using this rate against the rate of salt supply, this study redefines the conventionally accepted interpretation of upward-narrowing, upward-widening and columnar diapirs. Upward-narrowing diapirs form when the rate of salt supply is less than the rate of sediment accumulation multiplied by extension. Upward-widening diapirs form when the salt supply is greater than the rate of sediment accumulation multiplied by extension. Columnar diapirs form when the rate of salt supply is equal to the rate of sediment accumulation multiplied by extension. This new relationship explains the absence of columnar and upward-widening diapirs in passive margins where thin-skinned extension dominates, and emphasizes the significance of lateral movement (extension and shortening) in moulding the geometry of salt diapirs. © 1998 Elsevier Science Ltd. All rights reserved

INTRODUCTION

The parameters controlling the geometry of salt diapirs have been studied by many workers. The geometry of up-building diapirs rising through viscous overburden depends on the viscosity ratio between the source layer and its overburden (Ramberg, 1967; Whitehead and Luther, 1975; Woidt, 1980; Schmeling, 1987; Jackson and Talbot, 1989; Jackson *et al.*, 1990). By contrast, the geometry of diapirs down-built in brittle overburdens has been attributed to the rates of aggradation relative to the rate of diapiric rise (Barton, 1933; Seni and Jackson, 1983; Vendeville and Jackson, 1991; McGuinness and Hossack, 1993; Jackson *et al.*, 1994; Talbot, 1995).

Vendeville and Jackson (1991), McGuinness and Hossack (1993) and Talbot (1995) used different plots to illustrate how the rates of diapiric rise and aggradation affect the geometry of salt diapirs. In their plots of rate of aggradation vs rate of diapiric rise, Vendeville and Jackson (1991) distinguished three end-members of diapirs; first, upward-narrowing diapirs that form when rapidly deposited overburden onlap the salt; second, columnar diapirs which form when strata uplap against vertical diapir flanks during moderate deposition of overburden; and, third, upward-widening diapirs that form when salt extrudes and toplaps slowly deposited overburden (Fig. 1).

Based on unpublished data of Vendeville and Jackson (1993), McGuinness and Hossack (1993) presented two plots illustrating the effects of rate of sediment accumulation, rate of salt supply, and extension rate on the angle of dip between the margin of allochthonous salt sheets and the encasing sediments. McGuinness and Hossack (1993) suggested that ramps in the base salt record episodes of relatively rapid sedimentation, whereas low angle base salt (flats) mark periods of slower sedimentation. Talbot (1995) used R'/A' ratios to define the dip between the salt and its overburden.

This study emphasizes the importance of representing the evolution history of a diapir by three plots where all of the six parameters (sediment accumulation, salt supply, erosion, dissolution, extension and shortening rates) are incorporated into the conventionally moulding plots for diapirs. It also introduces a new factor (the rate of extension multiplied by sediment accumulation $(E{\cdot}A)'$) which plays a significant role in defining upward-narrowing, upward-widening and columnar diapirs.

MOULDING PARAMETERS

Jackson and Talbot (1991) listed eight rates relevant to salt tectonics. These are: aggradation rate of overburden (A'); dissolution rate of salt (D'); extension rate of overburden or salt (E'); lateral injection rate of salt structure (I'); progradation rate of overburden (P'); gross rate of salt flow upward (F'); net rate of increase in relief of salt structures (R'); and shortening rate (S'). McGuin-

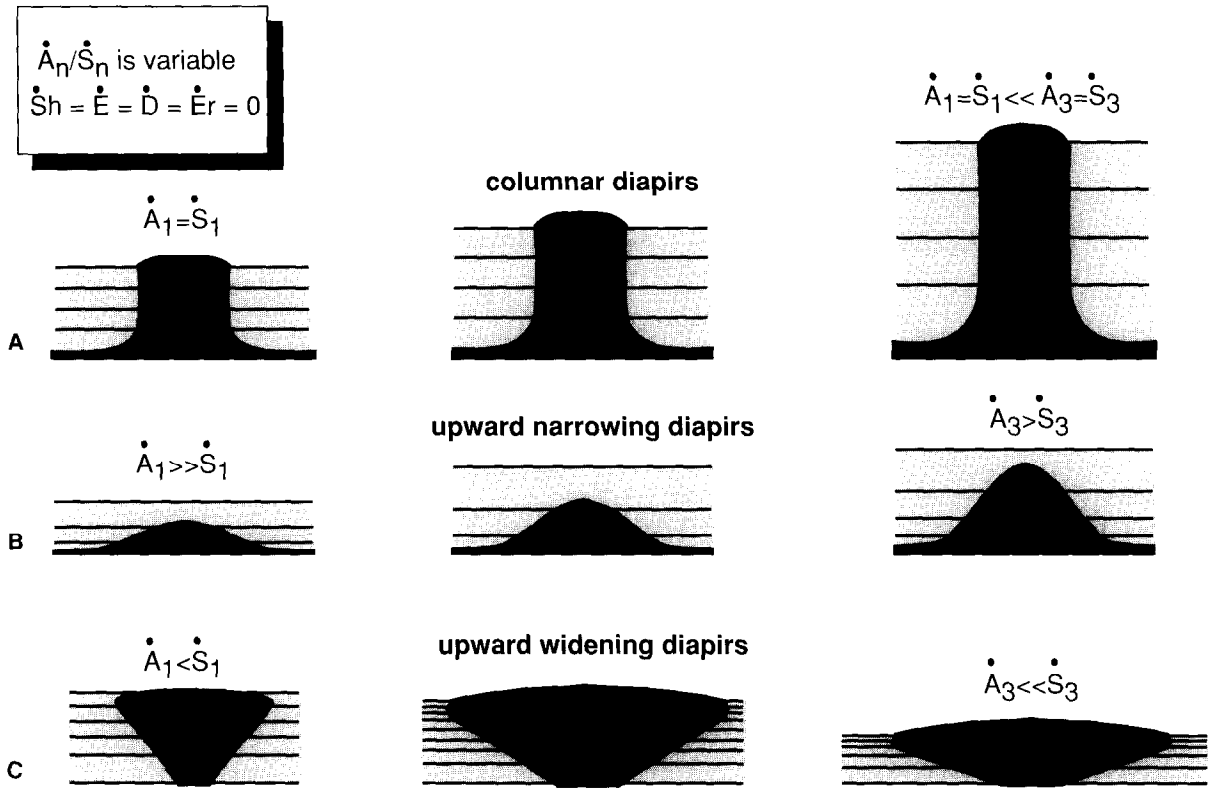

Fig. 1. Schematic representation of the geometry of diapirs formed at three end-members for the rate of sediment accumulation (A') and rate of salt supply (S'). (a) When $A' = S'$ columnar diapirs develop. At equally higher A' and S' taller columnar diapirs form. (b) Upward-narrowing diapirs form when the rate of sediment accumulation (A') outpaces the rate of salt supply (S'); and (c) upward-widening diapirs form when the rate of salt supply (S') outpaces the rate of sediment accumulation (A'). Modified after Vendeville and Jackson (1991). These relationships are true only when the rates of shortening (Sh'), extension (E'), dissolution (D') and erosion (Er') are assumed to be zero or insignificant.

ness and Hossack (1993) used the rate of salt supply (S') to cover both the rate of rise of diapirs (R') and rate of upward flow of salt (F'). As the rate of increase in relief of salt structures (R') is directly proportional to the rate of salt flow upward (F'), the approach by McGuinness and Hossack (1993) is sound. Overburden accumulation could be due to different end-members of the spectrum between aggradation and progradation. Unless it is obvious that one of these two processes is responsible for the deposition of the overburden, rate of sediment accumulation (A') would be an appropriate parameter to replace both aggradation and progradation rates. To avoid errors that occur due to distinguishing rates of aggradation (A') from rates of progradation (P'), in this paper, like McGuinness and Hossack (1993) and Talbot (1995), both processes are considered together under the single label of the rate of sediment accumulation (A'). Here, A' is used as the rate of sediment accumulation at a given time after compaction without including the thickness of the salt layer. In order to standardize the terminology, rates of salt supply (S'), sediment accumulation (A'), extension (E'), shortening (Sh'), dissolution (D') and erosion (Er') are used. From these rates, a new rate, namely the rate of the product of extension multiplied by sediment accumulation, $(E{\cdot}A)'$ is presented to be used against the rate of salt supply (S') to redefine the geometry of salt diapirs. It is important to emphasize that when one of the elements of the above rate is insignificant (e.g. when there is zero extension), in order not to end up with a zero product of $(E{\cdot}A)'$, only the other element is considered. For example, when extension (E) is insignificant only sediment accumulation (A) is taken into account, and vice versa.

Recently, Talbot (1995) used the logarithmic ratios of R'/A' and/or A'/R' to predict the tangent of the dip of the salt contact with its overburden and explain the geometry of the resulting structures. In the study by Talbot (1995) R is salt rise minus dissolution and A is net accumulation of overburden. Plots of the R'/A' ratio obscure the size and absolute growth rate of the structure. If we only consider the rates of sediment accumulation and salt supply as moulding parameters for the geometry of salt diapirs, the plots by Vendeville and Jackson (1991) and McGuinness and Hossack (1993) are more appropriate as they show that when both S' and A' are equal to, say, 2 mm y^{-1} each the columnar diapir is twice as tall and rises faster than when both rates have a value of 1 mm y^{-1} (Fig. 1a). In the plot by Talbot (1995) both these cases are represented by a columnar diapir regardless of their size and growth rate. The same is true for upward-narrowing and upward-widening diapirs. In these two cases also, the A'/S' ratio can produce similar

diapirs with the same contact dip but of different sizes.

Ratios are unitless and discard the rate at which the diapir rose or the sediments accumulated, which are important parameters for studying hydrocarbon maturation, migration and entrapment. Plots of ratios discard the time aspect of the processes that influence the moulding of a diapir. Moreover, if lateral movements are added to moulding parameters for salt diapirs, many other ratios (for example, between the rates of extension, shortening, salt supply and sediment accumulation) need to be defined.

Included in the conventional plots are the rates of dissolution of salt (negative salt supply), erosion of overburden (negative sediment accumulation), regional extension and shortening adds details to the evolution history of the salt diapir. Rates of sediment accumulation and salt supply alone cannot explain the different geometries of salt diapirs. For example, it is suggested that columnar diapirs form when the rates of sediment accumulation and salt supply are equal (Vendeville and Jackson, 1991). However, in addition to columnar diapirs that form when S' and A' rates are equal, if the rate of extension multiplied by sediment accumulation $(A \cdot E)'$ is compared to the rate of salt supply (S'), columnar diapirs can be produced in two more cases even when A' and S' are not equal (Fig. 2). When A' is insignificant, and E' is equal to S', widening columnar diapirs form (Fig. 2b), and self-similar columnar diapirs (Fig. 2d) form when rate of salt supply is equal to the rate of sediment accumulation multiplied by extension $(A \cdot E)'$.

Figure 3 shows all six rates (S', A', Er', D', E' and Sh') on a single plot. Although only the end-members are shown, endless examples can be plotted. Because plots like Fig. 3 may be too complicated, plots of pairs of parameters are recommended. Each of these plots would represent two of the six parameters mentioned above (Fig. 4). Each profile of a diapir should be represented by three plots that represent the main parameters that influenced its evolution (Fig. 4). When three-dimensional data are available these plots yield four-dimensional geometrical evolution of the structure. These three plots are: a plot for rate of salt supply vs the rate of sediment

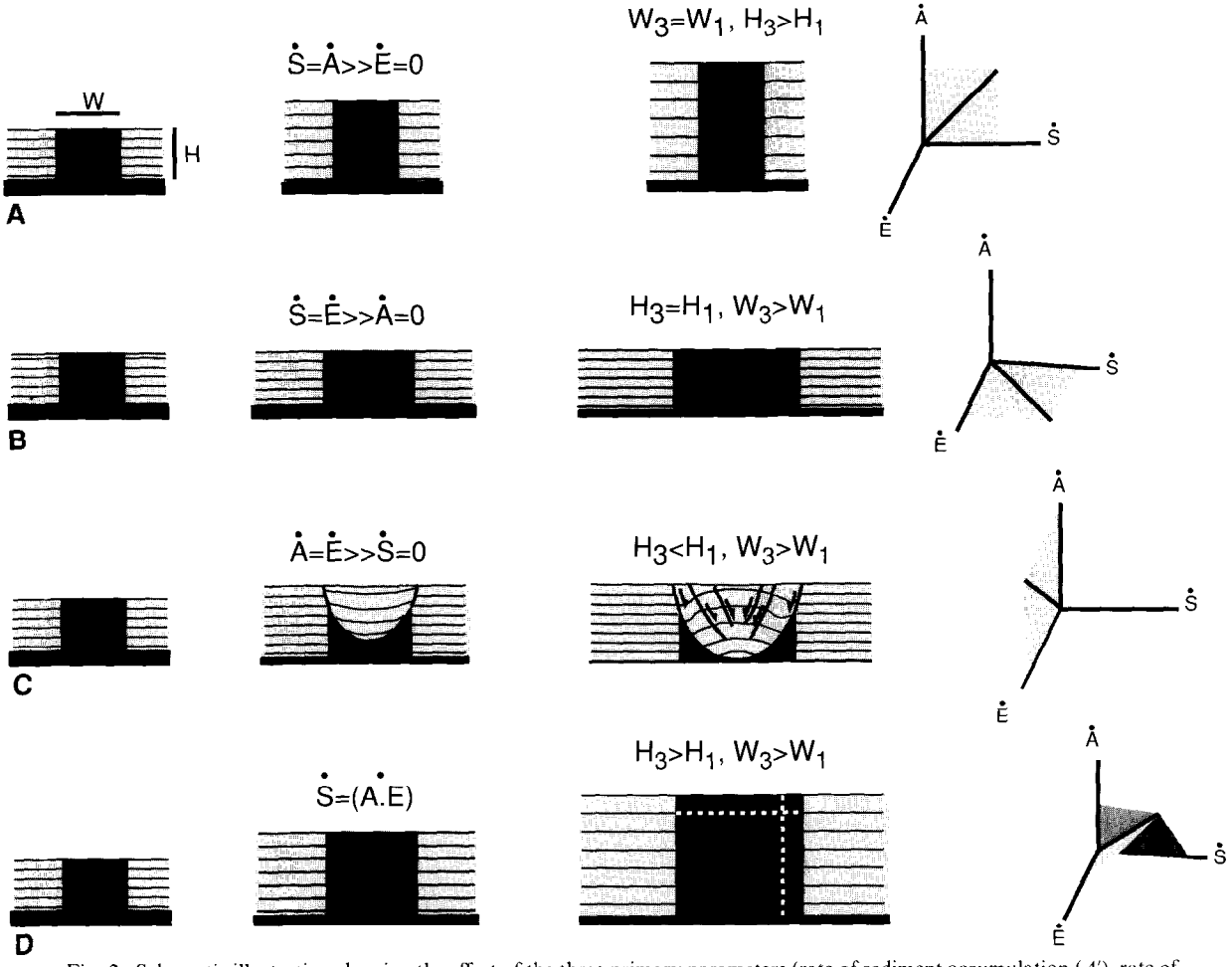

Fig. 2. Schematic illustration showing the effect of the three primary parameters (rate of sediment accumulation (A'), rate of salt supply (S') and extension rate (E')) on moulding columnar diapirs. (a) When E' is zero, equal S' and A' rates mould tall columnar diapirs. (b) When A' is zero, equal E' and S' rates mould wide columnar diapirs. (c) When S' is zero, equal A' and E' rates mould falling diapirs. (d) When all the three parameters are active and the rate of salt supply (S') is equal to the rate of extension multiplied by sediment accumulation $(E \cdot A)'$ self-similar columnar diapirs form. These diapirs grow both in width and height. In these drawings the starting structure is a small columnar diapir. S'–A'–E' plots are shown to the right for each case. W and H are the width and height of the diapirs, respectively.

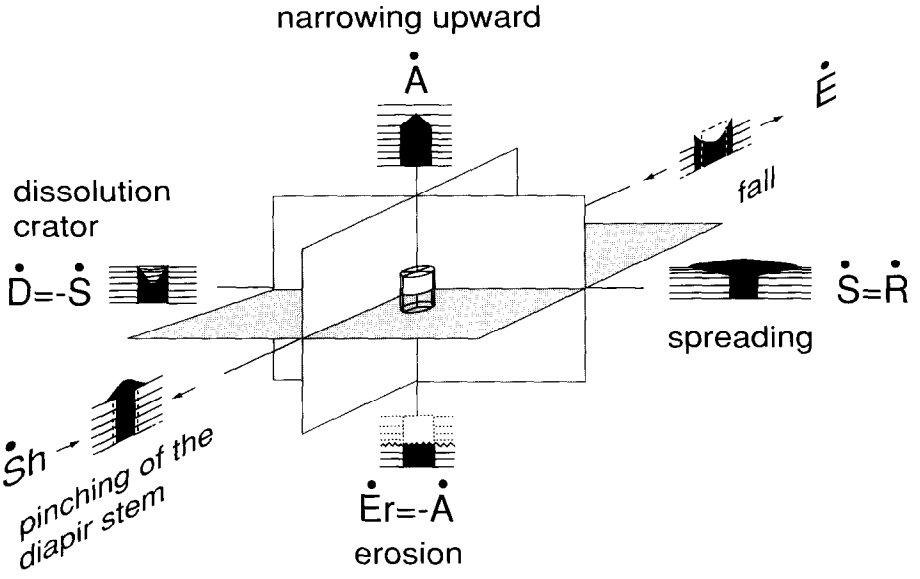

Fig. 3. A six-parameter plot of the rates that mould the geometry of salt diapirs. In this plot only the end-member geometries are shown. The cylinder in the centre of the plot is the starting geometry of a diapir prior to applying the six parameters. Dashed lines outline a previous geometry. If applied to a profile of a salt diapir, this plot shows only the two-dimensional evolution history of the diapir.

accumulation; a second plot for rate of salt supply vs the rate of lateral movement (extension and/or shortening); and a third plot for the rate of lateral movement (extension and/or shortening) vs the rate of sediment accumulation (Fig. 4). These three plots are represented by the Z–X, X–Y and Z–Y planes, respectively, in Fig. 3.

BACKWARD MOULDING

The present geometry of salt diapirs is the result of interaction between the six parameters (S', A', D', Er', E' and Sh') during the evolution of the diapir. Therefore, it should be possible to deduce the relative magnitudes of moulding parameters (S', A', D', Er', E' and Sh') from the geometry of salt diapirs. This is possible if at least two of the moulding rates is relatively well constrained. If one of these parameters is zero, for example in profiles with diapirs not being influenced by lateral movement (extension or shortening), deducing the moulding history would be relatively easier. In this case, if only one of the two remaining parameters is well constrained (e.g. rate of sediment accumulation), the other can be deduced relatively easily from the geometry of the diapir. Nevertheless, even in such cases the evolution history of the area and the three-dimensional geometry of the structure should be taken into account.

Recently, Talbot (1995) inferred histories of moulding ratios (A'/R') from single profiles of individual diapirs from the East Texas Basin and the Gulf of Mexico. The backward moulding approach applied by Talbot (1995) is worth elaborating upon by adding the effect of the other parameters (E', Sh', D' and Er') and including the regional geology. Then the plots of S' vs E' and A' vs E' for the diapir profiles should be included in the backward moulding. In addition to that, as the S'–A', S'–E' and A'–E' plots of a non-axisymmerical diapir vary with profile (Fig. 4), the three-dimensional aspect of salt structures should be taken into account during backward moulding. Because rock salt flows due to differential loading (both tectonic or sedimentational), it is likely that resulting structures would have cross-sectional geometries that vary with the azimuth of the line of section (Figs 4 & 5). Model diapirs triggered by extension show that the A'–S' plots vary significantly in two cross-cutting profiles. In profiles parallel to the extension direction, extension plays an important role in moulding the geometry of the diapir (see below). Therefore, two other plots, i.e. A' vs E' and S' vs E', should be produced (Fig. 4). On the other hand, in a centred profile perpendicular to the extension direction, where extension is negligible, A' vs S' plots are sufficient to represent the two-dimensional moulding history of the diapir in that profile (Fig. 4). It is not possible to correctly deduce the full moulding history of a three-dimensional salt diapir from a single two-dimensional profile, which gives only a two-dimensional evolution history of the structure.

One or more of the parameters that mould a diapir may vary both in time and space. If the dip of the salt contact is used to derive the A'–S' plots, as suggested by McGuinness and Hossack (1993) and Talbot (1995), within the same profile, an asymmetric diapir overhang would yield different rates of sediment accumulation and/or salt supply on either sides (Figs 6 & 7). McGuinness and Hossack (1993) attributed steep ramps in the base of salt to episodes of relatively rapid sediment accumulation, and low angles in base salt (flats) to periods of slower sediment accumulation. But ramps on one side

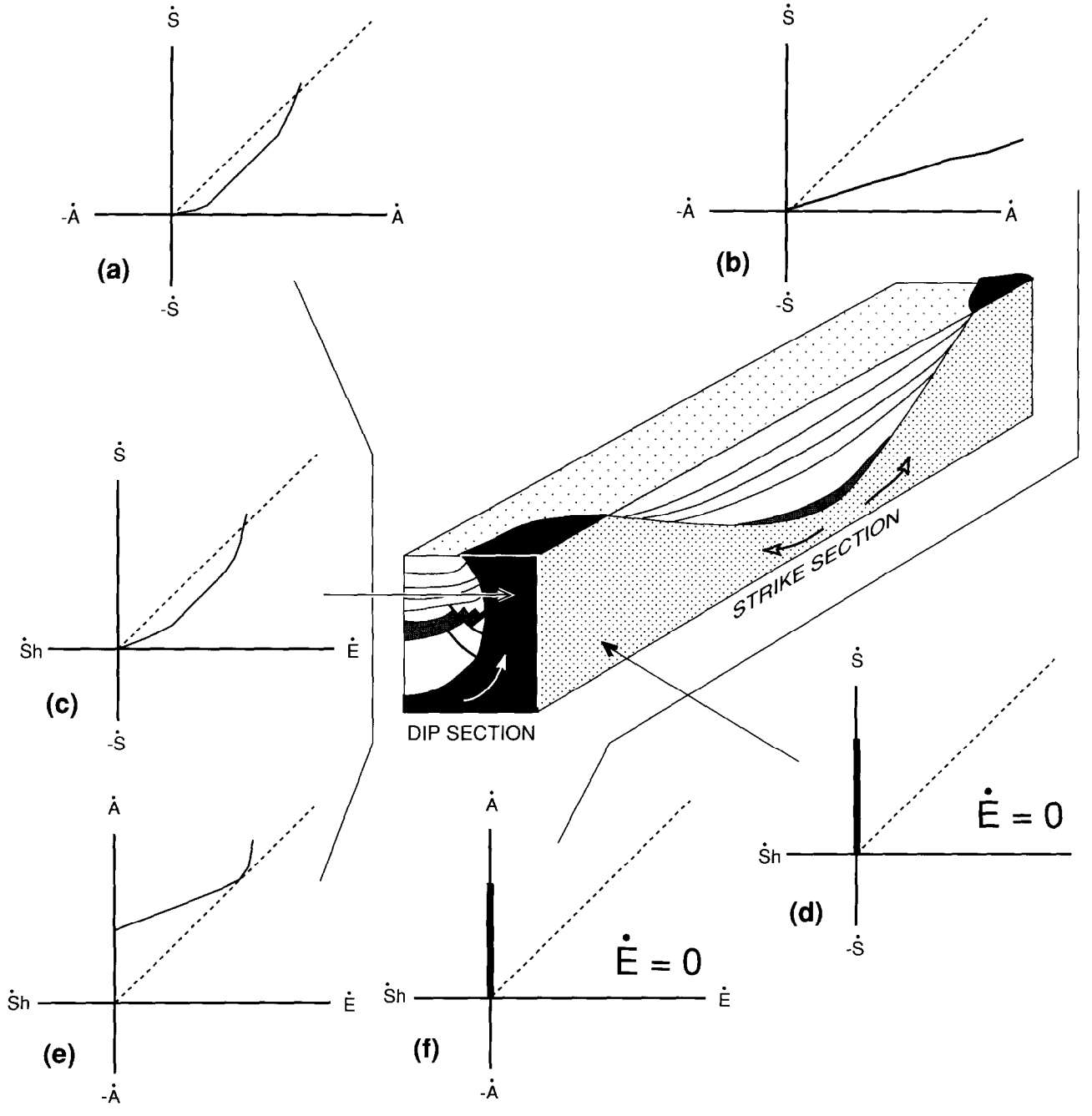

Fig. 4. A block diagram of the late stage of diapir growth. (a) & (b) Plots of the rate of salt supply (S') vs the rate of sediment accumulation (A') for two different profiles of the same diapir in the block diagram. (c) & (d) Plots of the rate of salt supply (S') vs extension rate (E'). (e) & (f) Plots of the rate of sediment accumulation (A') vs extension rate (E') for the same two profiles. The three plots (a), (c) & (e) together represent the evolution history of the diapir in dip section for they account for the parameters that influence the geometry of the structure in this section. In the strike section the evolution history of the same structure is represented by plots (b), (d) & (f), which are different to their equivalents in (a), (c) & (e). In (d) & (f) plots the curve is represented only by the S' axis because extension in this section is zero. Shortening (Sh'), dissolution (D') and erosion (Er') rates are not accounted for in any of these plots as they are equal to zero. The block diagram is modified after Jackson *et al.* (1994).

can be contemporaneous with flats on the other side of the same profile of a salt structure with a single rate of supply (Fig. 6). In other words, time-related ramps and flats could also relate in space. The steeper dip on the right-hand side of the structure in Fig. 6 suggests a relatively faster rate of sediment accumulation than rate of salt supply. The asymmetry, in general, results from spreading of salt faster down-dip (for example, basinward spreading or spreading over a fault scarp) while the up-dip side is buried. The asymmetry is due to the slope, which in turn is due to a lower rate of sediment accumulation on the down-dip side, a locally higher

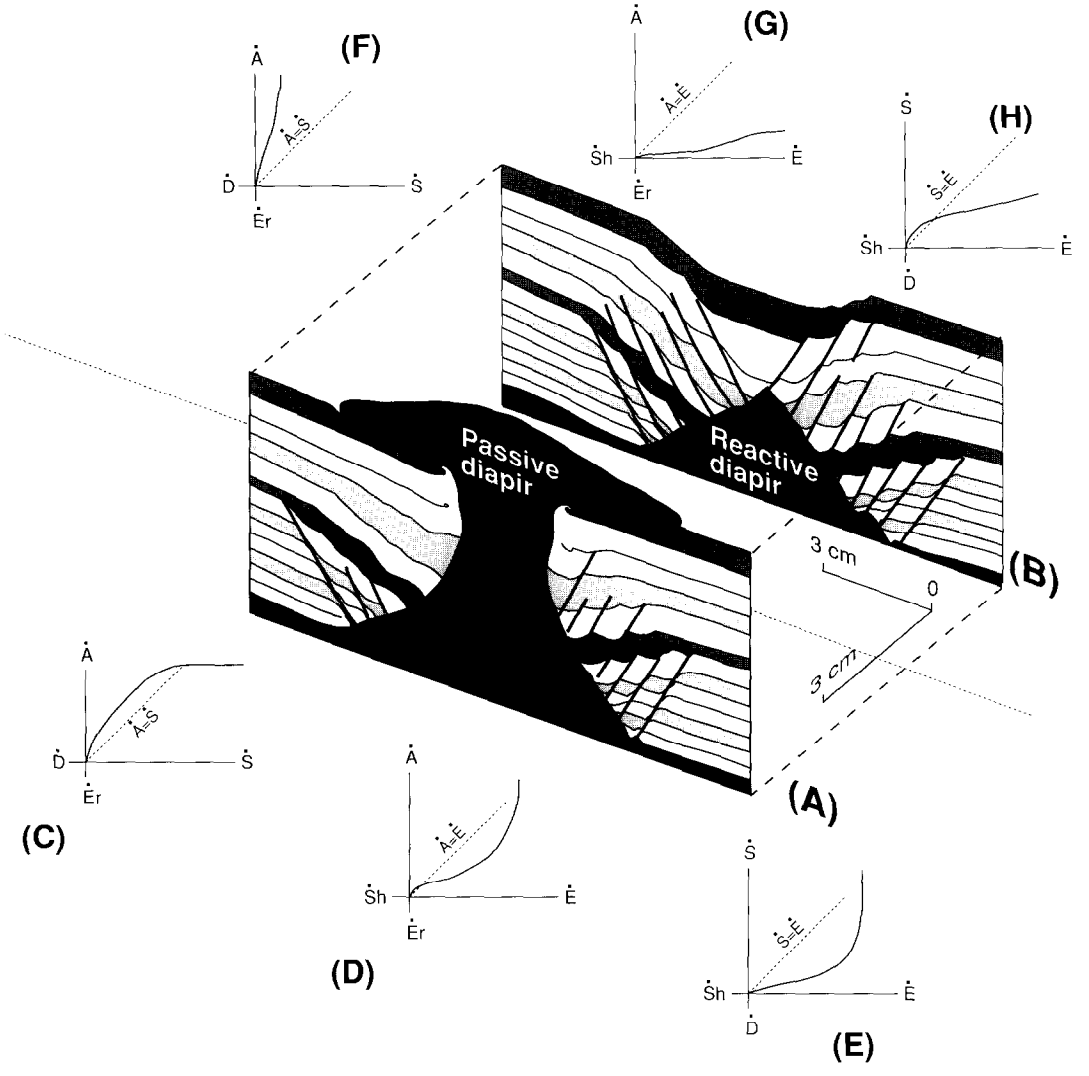

Fig. 5. (a) & (b) Line drawing of two parallel profiles of an analogue model, formed by regional extension, illustrating the change of geometry of diapirs with profile (modified after Vendeville and Jackson, 1992a). (c)–(e) are the three moulding plots (rate of sediment accumulation (A') vs rate of salt supply; rate of sediment accumulation (A') vs extension rate (E'); and rate of salt supply (S') vs extension rate (E'), respectively) for the passive diapir in (a). (f)–(h) are the equivalent plots for the reactive diapir in (b). Note that, although the model was extended equally, due to differential loading and 'salt' flow between these two diapirs, which are connected in space and time, the equivalent plots are considerably different.

subsidence rate due to salt withdrawal and/or due to a regional cooling and/or due to progradation that drives the salt in the transport direction. Salt supply through a diapir stem may be constant but, due to the differential spreading, the relative supply rate may vary on either side (in a profile) of the structure. Consequently, A'–S' plots differ on each side because of different rate of sediment accumulation and the presence of a basinward slope (Fig. 6). Also, due to differential spreading of the salt supply, the side with larger horizontal/vertical flow ratio is buried, while the side with smaller horizontal/vertical flow ratio keeps up with the same rate of sediment accumulation (Fig. 7). In the Nordkapp Basin the slope is concentric to the basin centre and the salt diapirs spread broader overhangs basinwards (Koyi *et al.*, 1993). The salt diapir in Fig. 7(a) is asymmetric and, therefore, there are two moulding curves relative to either side of the structure (Fig. 7b & c). To illustrate the effect of erosion on the moulding of salt diapirs simplified S' vs A' plots are prepared from a profile of an asymmetric diapir in the Nordkapp Basin (Fig. 7).

EFFECT OF EROSION

In many basins with salt diapirs episodes of erosion have removed large volumes of either sediments and/or salt (e.g. Danish Basin, North Sea, Nordkapp Basin). Erosion phases can be pre-, syn- and post-diapirism. Consequently, they are likely to have influenced both the rising rate of the diapir and rate of sediment accumulation, and, hence, the moulding history of the diapirs.

Pre-diapiric erosion may not influence the geometry of

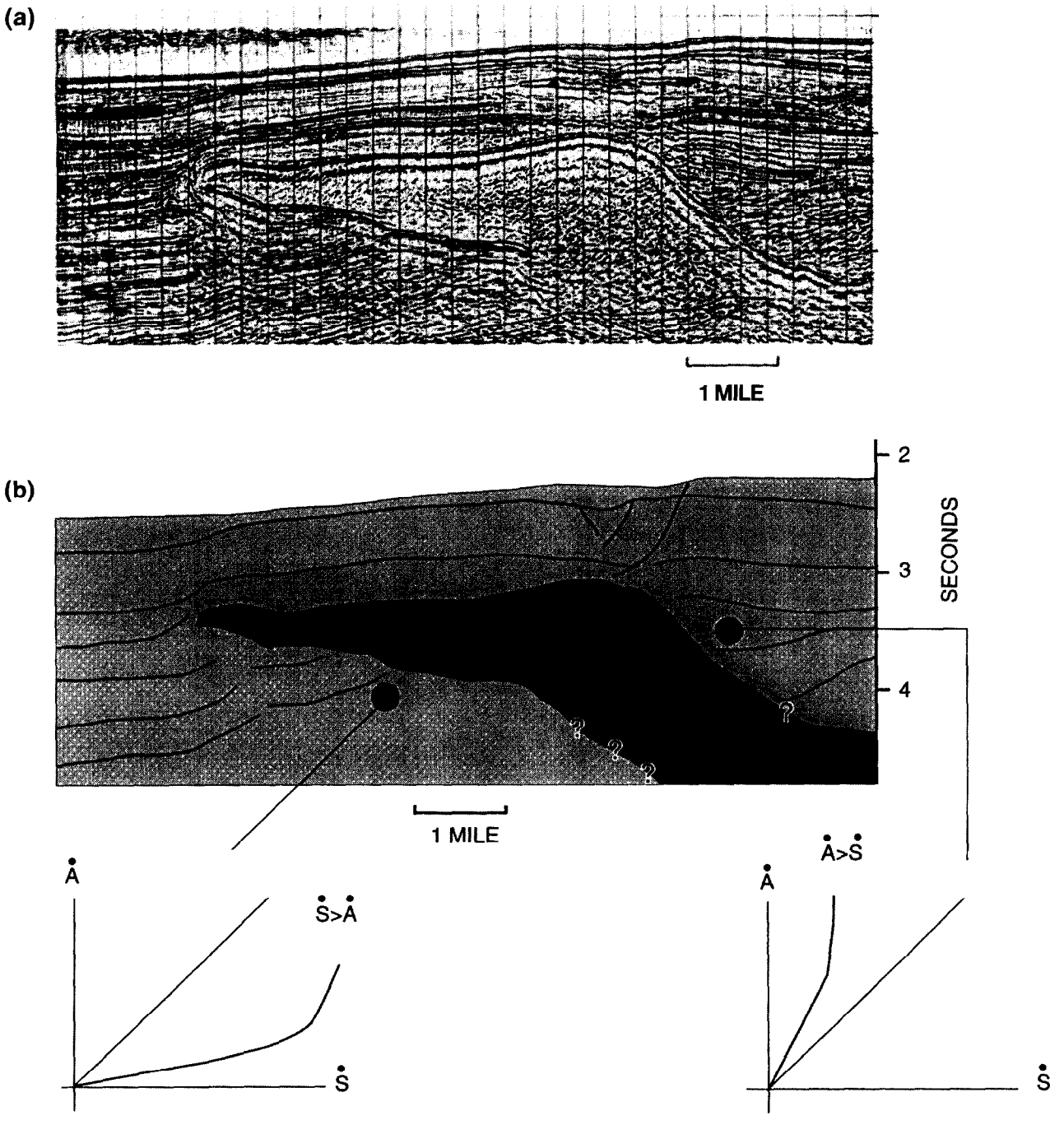

Fig. 6. (a) Seismic line (after Nelson, 1991) and (b) its line drawing showing a salt sheet in the Gulf of Mexico. Judging from the salt contact with its overburden on either sides of the structures, there could be two different plots of the rate of sediment accumulation (A') vs the rate of salt supply (S') representing the moulding history of these two sides.

a future diapir, but it thins its overburden which, in the presence of another triggering mechanism (e.g. extension, differential loading), may assist intrusion. Syn-diapiric erosion erodes overburden units and salt from a rising diapir. Here, again, erosion thins the overburden units above the crests of salt domes and aids piercement. Consequently erosion may influence the geometry of the diapir as it forms because it reduces sedimentation rate. In fact, many salt diapirs which have developed through a pillow stage owe their piercement to erosion and thinning of their overburden that was elevated above their domal crest. This erosion has probably aided transition from the pillow stage to diapiric stage and piercement (Trusheim, 1960).

Post-diapiric erosion (erosion which happens during a period when the diapiric growth is very slow or insignificant) can also lead to changing the geometry of a diapir after it has formed. For example, the salt diapirs of the Nordkapp Basin have experienced several phases of erosion both during an intermediate stage (Jurassic) and at later stages (Cenozoic) of their evolution. The amount of Late Tertiary erosion in the Nordkapp area is

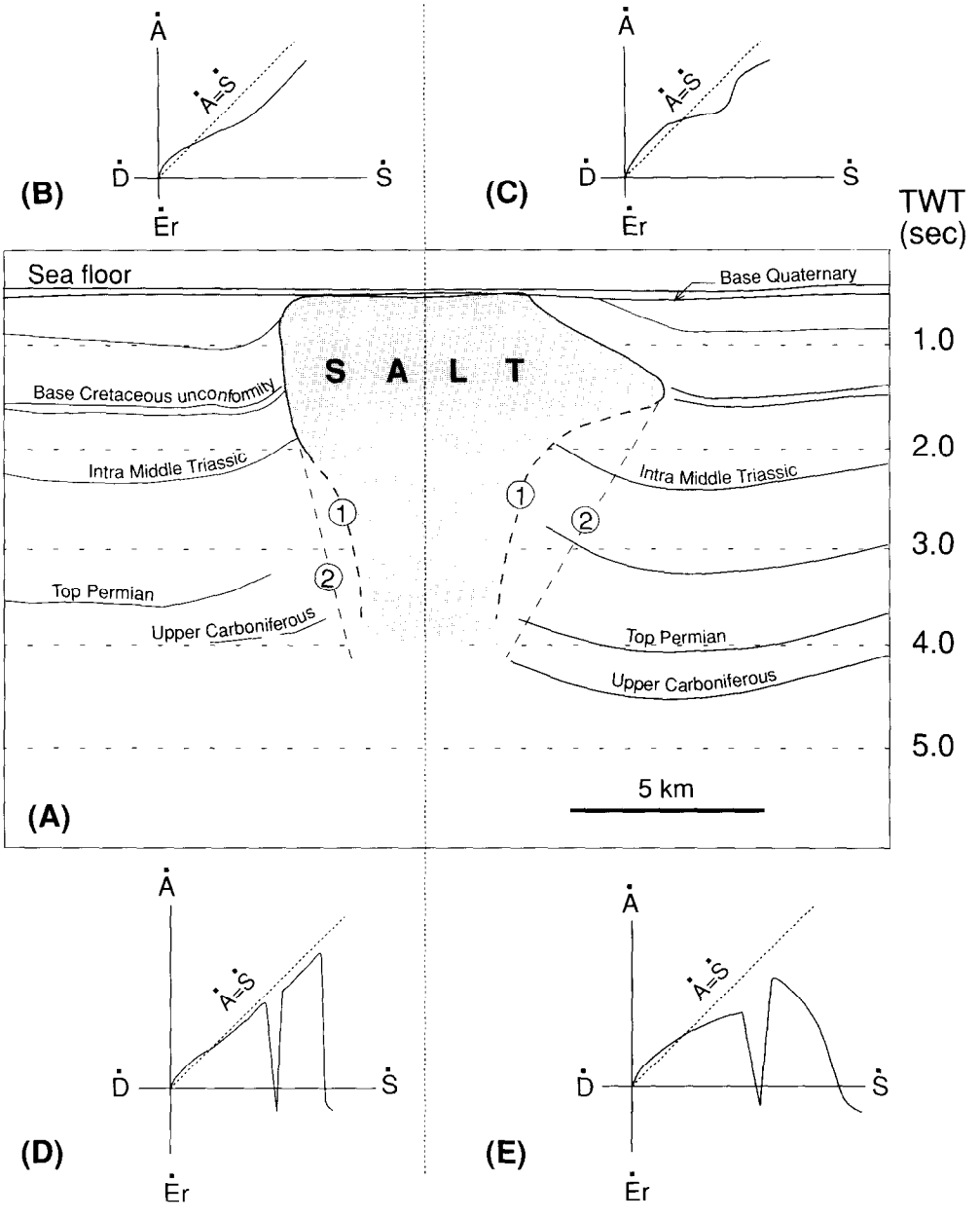

Fig. 7. (a) Line drawing of a seismic line showing a salt diapir of the Nordkapp Basin with an asymmetric overhang (modified after Koyi *et al.*, 1993). (b) & (d) are plots of the rate of sediment accumulation (A') vs rate of salt supply (S') deduced from the left side of the diapir. The difference between these two plots is that in (d), which is the correct two-dimensional plot of this side of the diapir, the erosion history is accounted for but not in (b). (c) & (e) are the equivalent plots for the right side of the diapir. A similar difference is seen here due to neglecting erosion in (c). These plots do not represent the complete evolution history of the diapir as they are prepared from only one profile. They illustrate the significance of erosion on the evolution history of a diapir in two dimensions. The plots are deduced from the geometry of the diapir.

estimated to be in the order of 1000–1700 m (Nyland *et al.*, 1992; Richardsen *et al.*, 1993). The majority (90%) of the salt diapirs in the Nordkapp Basin subcrop below the sea floor. This could be attributed to the later erosion phases, which have thinned and/or removed the overburden units above the diapir crest.

During the low sedimentation period in the Jurassic many salt diapirs in the Nordkapp Basin developed overhangs broader than their feeding stems that spread asymmetrically basinward (Koyi *et al.*, 1993) (Fig. 7a). It is probable that these overhangs were subjected to dissolution at this time (Koyi *et al.*, 1993). The rapid increase in rate of sediment accumulation during the Cretaceous (Richardsen *et al.*, 1993) covered the existing diapir overhangs in the Nordkapp Basin. The second phase of erosion that took place during the Late Tertiary (Riis and Fjeldskaar, 1992) removed up to 1000 m of the overburden units. If erosion is added to S'–A' plots of either side of the diapir, two new plots can be drawn from the geometry of the diapir plus the erosion history of the area (Fig. 7d & e). This example demonstrates the importance of accounting for the regional history of the area when backward moulding the geometry of salt structures.

LATERAL MOVEMENT

Most diapirs have experienced some degree of extension or shortening (or both) during their evolution. Salt diapirs occur in both extensional (e.g. North Sea, Kwanza and Santos Basins) and compressional areas (Perdido fold belt, Gulf of Mexico and Zagros mountain belt, Iran). Vendeville and Jackson (1992a,b) argued that regional extension originally promotes piercement by tectonically induced differential loading, but it also impedes upward salt flow by horizontally stretching the diapir. As described by Vendeville and Jackson (1991) and McGuinness and Hossack (1993), parallel with the rates of salt supply and sediment accumulation, extension influences the geometry of salt structures. This concept can be specified further by distinguishing the influence of pre-, syn- and post-diapiric lateral movements on moulding the geometry of salt diapirs and introducing a new rate (rate of the product of extension multiplied by sediment accumulation ($E \cdot A$)') which defines the upward-narrowing, upward-widening and columnar diapirs.

Extension

Thin- and thick-skinned extension trigger diapirism by faulting overburden units and creating the space for the diapirs to occupy (Vendeville and Jackson, 1992a,b; Koyi *et al.*, 1993; Nalpas and Brunn, 1993). In this section, in order to study the role of extension in moulding the geometry of salt diapirs, pre-, syn- and post-diapiric extension are distinguished.

Pre-diapiric extension, which takes place before the onset of diapirism, aids piercement by thinning pre-existing overburden units that eventually differentially loads the underlying salt and triggers piercement. This case is well studied by Vendeville and Jackson (1992a) who showed that extension thins overburden units by faulting to initiate diapirs growing from the reactive stage to actively intruding the overburden (active stage). The geometry of diapirs resulting from pre-diapiric extension is strongly governed by the extension and the faults in its overburden (Fig. 8a & b).

Syn-diapiric extension, which takes place during diapirism, thins synchronous sediments by faulting and consequently assist piercement. However, in general, extension widens the space which the diapir needs to fill. Even if the source layer is not depleted, if it is not able to keep pace with extension the salt supply will not be enough to fill the 'additional' space created by extension and support the vertical flow. In this case, the diapir sags (Vendeville and Jackson, 1992b) and is eventually buried beneath the accumulating sediments. The effect of syn-diapiric extension is illustrated by using the analogue models of Lin (1992). Lin (1992) prepared and described a series of analogue models of a ductile substrate deforming beneath layers of loose sand of different thicknesses deposited at different times. In general, these models simulated syn-diapiric extension. In this paper only three of those models (referred to as experiments 39, 47 and 60 and reproduced in Fig. 9) are analysed and used to illustrate the influence of syn-diapiric extension on the moulding of the geometry of diapirs. In these three models loose sand layers were 'deposited' at different rates on a 1 cm thick Newtonian viscous layer (viscosity $= 3 \times 10^4$ Pa.s, density $= 970$ kg cm^{-3}). The material used for the viscous layer was polydimethylthyloxane, which is a transparent silicone polymer gum manufactured under the code SGM36 by Dow Corning. Deformation in these models was initiated by allowing the model to spread at one open end. The restored profiles produced by Lin (1992) are used to calculate and plot the extension rates for each of these three models (Fig. 9). However, the bulk extension rates of each model were calculated by comparing the initial and final stages of the models. The plots show that extension rate changes with time within the same model. It decreases with time as the viscous layer thins resulting in an increase of the effect of drag force along the bottom boundary of the model. Below, these three models are described and analysed.

In experiment 39, which was simulating fast rate of sediment accumulation (1 cm h^{-1} $= 2.7 \times 10^{-3}$ mm s^{-1}), the bulk extension rate was as high as 2 cm h^{-1} (5.5×10^{-3} mm s^{-1}) (Fig. 10a). The high extension rate is attributed to the greater load exerted by the thicker overburden on the underlying ductile substrate to flow laterally towards the open end of the model. Here, although the bulk extension rate was twice as large as the rate of sediment accumulation, it cannot stretch and weaken the rapidly accumulating overburden sufficiently to allow reactive diapirs to initiate from the underlying source layer. The source layer instead segmented into 'salt' rollers separated by rotated overburden blocks (Fig. 9a).

In experiment 47, which simulated a moderate rate of sediment accumulation (0.25 cm h^{-1} $= 6.9 \times 10^{-4}$ mm s^{-1}) that was 4 times smaller than that of experiment 39, the bulk extension rate was as high as 1.78 cm h^{-1} (4.9×10^{-3} mm s^{-1}) (Fig. 10b). Here, the extension rate stretched and thinned the overburden sufficiently to initiate reactive diapirs (Fig. 9b). However, due to relatively fast accumulation of overburden layers, these diapirs never reached the active stage of piercement. Instead, as extension continued, the diapirs broadened with time and possessed an upward-narrowing geometry (Fig. 9b). It is important to emphasize that the upward-narrowing geometry of the diapirs is not only due to a higher rate of sediment accumulation relative to the rate of salt supply but also due to the influence of the overburden faults formed during extension (Fig. 9b).

In experiment 60, which simulated slow rate of sediment accumulation of 0.125 cm h^{-1} (3.4×10^{-4} mm s^{-1}), the bulk extension rate was 1.06 cm h^{-1} (2.9×10^{-3} mm s^{-1}) (Fig. 10c). At the early stages of this experiment, several diapirs started to rise below

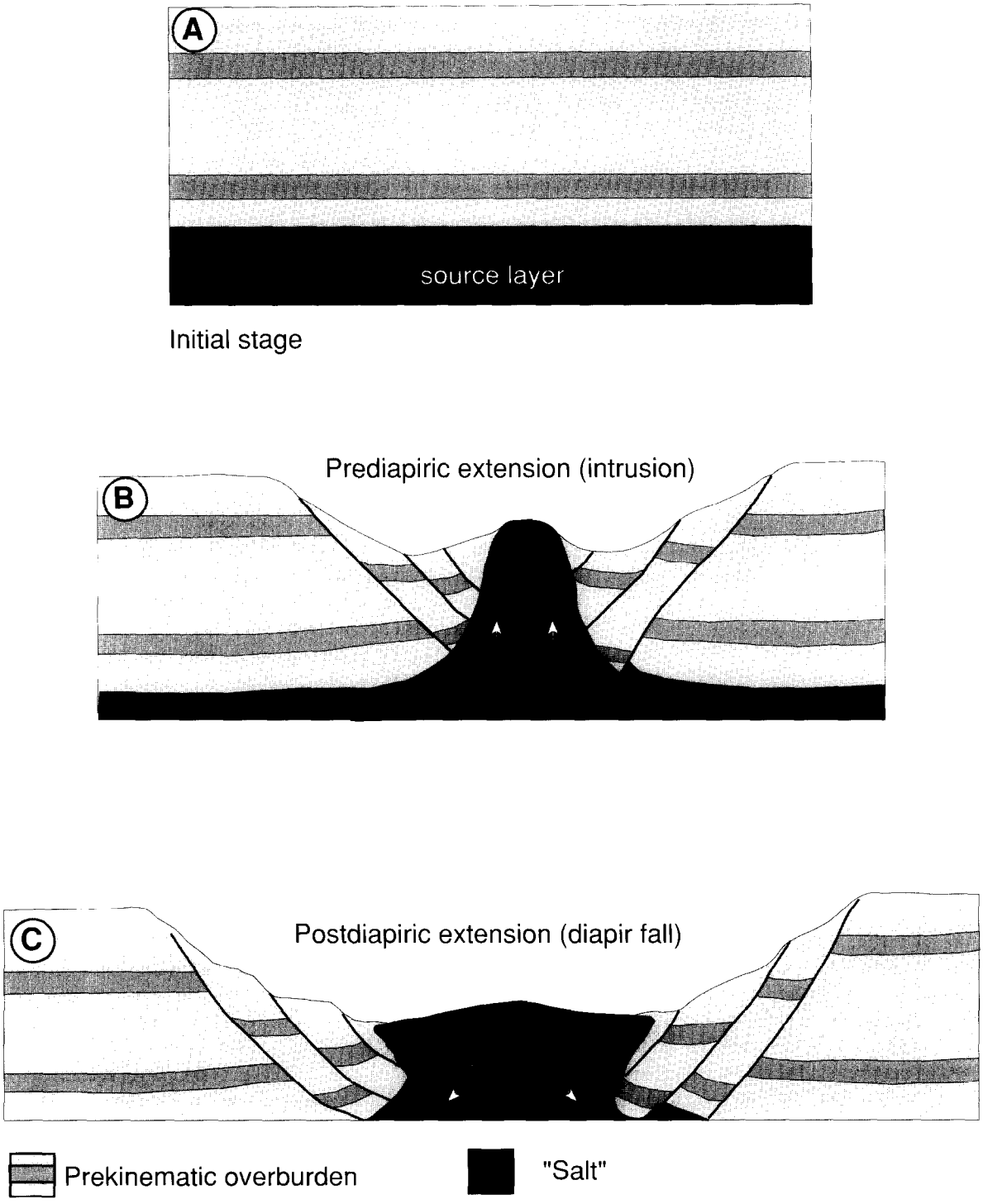

Fig. 8. Line drawing of (a) the initial and (b) the deformed stage of reactive diapirs formed due to pre-diapiric extension. (c) A line drawing of (b) after continuous extension. This stage illustrates the effect of post-diapiric extension on a pre-existing diapir. Note that the diapir sags as its supply decreases. Based on analogue models by Vendeville and Jackson (1992a).

grabens defined by stair-stepped faults (Lin, 1992). Some of these diapirs can grow from the reactive stage to actively piercing their overburden and finally grow passively as new overburden units flanked their surfaced crests (Fig. 9c), whereas low relief diapirs sagged and subsided below depotroughs (Lin, 1992) (Fig. 9c). At later stages, the emergent passive diapirs were not flanked by faults in the overburden because extension rate was decreasing significantly (Fig. 10c). All the diapirs in this experiment possess upward-narrowing geometries. The few diapirs which kept up with sedimentation with their crests at the surface, also narrowed upward mainly because the salt supply decreased dramatically as the viscous layer depleted.

Post-diapiric extension, which takes effect after the diapir has intruded its overburden, could influence the

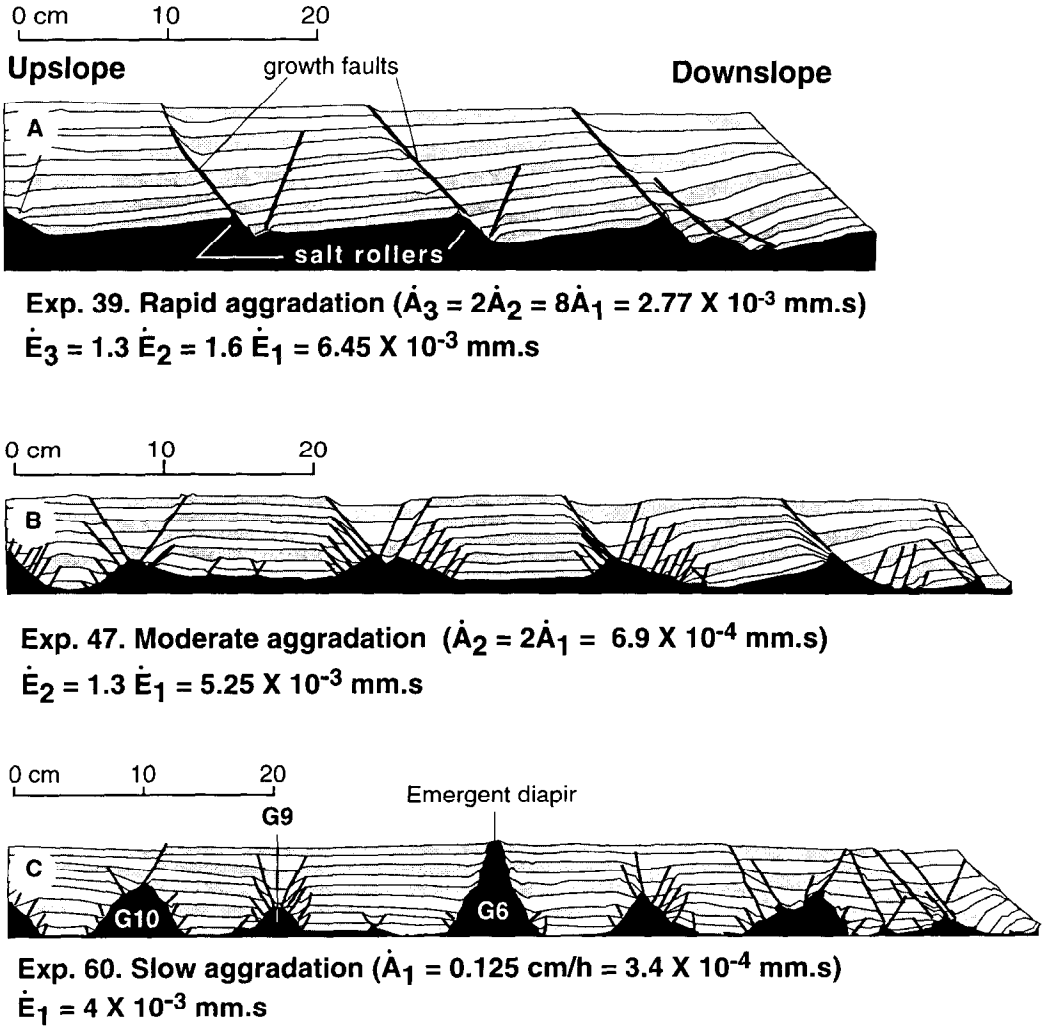

Fig. 9. Line drawing of three model profiles, modified after Lin (1992), illustrating the effect of aggradation and extension rates on the geometry of diapirs. (a) Model 39, where bulk extension rate is twice as much as the rate of sediment accumulation. (b) Model 47, where bulk extension rate is 7.5 times greater than the moderate rate of sediment accumulation. (c) Model 60, where bulk extension rate is more than 11 times greater than the slow rate of sediment accumulation. Note that only when the extension rate is significantly greater than the rate of sediment accumulation (b & c) can diapirs intrude their overburdens. Rates of salt supply and extension are measured for diapirs G6, G9 and G10 in experiment 60 in (c).

geometry of the diapir in different ways depending on the amount of the source layer left to feed the diapir and the rate of salt supply relative to the extension rate. In order to be able to fill the additional space created by the extension, and still be able to keep its crest at the same level, material supply to the diapir from below needs to be sufficient in both rate and amount. If no sediments are added the rate of salt supply must match the extension rate. If sedimentation is active simultaneously with post-diapiric extension the rate of salt supply needs to be equal to the rate of extension multiplied by sediment accumulation. Otherwise, the diapir widens and sags beneath the accumulating sediments. Sagging of diapirs due to extension is described in detail by Vendeville and Jackson (1992b) (Fig. 8c). On the other hand, post-diapiric extension aids piercement by thinning and faulting any overburden units above the crest of a diapir. If the rate of salt supply can keep up with the extension rate it can intrude through the faulted overburden units above its crest, otherwise the diapir sags and falls.

Shortening

In order to study the effect of pre-, syn- and post-diapiric shortening on moulding of diapirs, three analogue models were prepared. Each model consisted of a viscous layer of SGM36 simulating salt underlying overburdens of loose sand of different thicknesses. The sand layers were passively coloured to quantify model deformation.

In model 1, which simulated pre-diapiric shortening, a 1.3 cm thick viscous layer of SGM36 was buried under 1.3 cm thick layer of banded loose sand. The model was then shortened continuously at a rate of 1.8 cm h^{-1} (5×10^{-3} mm s^{-1}). As the model was shortened, both the source and overburden layers thickened tectonically.

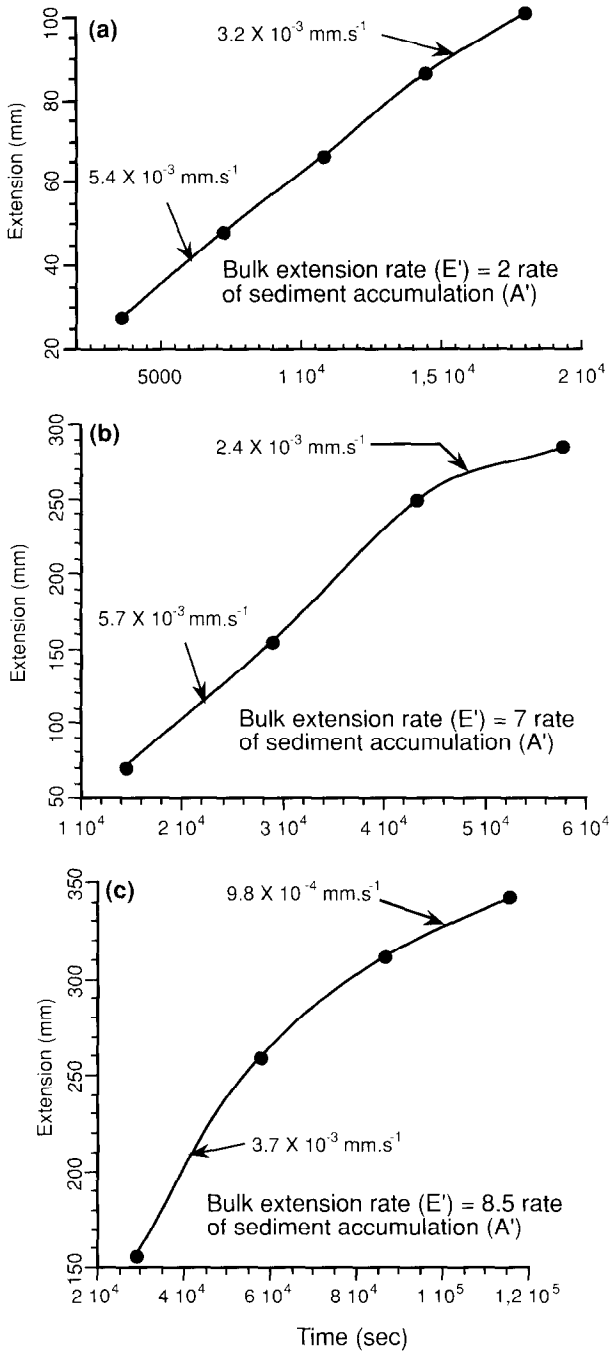

Fig. 10. Plots of extension with time for the three models described in Fig. 9: (a) model 39, (b) model 47 and (c) model 60. These plots were prepared restored profiles of the models from Lin (1992). Bulk extension rates were calculated by comparing the initial and final stages of the models.

An anticline cored by the viscous material formed in the overburden. As the shortening intensified, the forelimb of the fold overturned and ruptured. Consequently, the viscous material was pinched in the core of the anticlines and separated from its feeding source layer (Fig. 11a & b). No diapirs could penetrate the overburden units, which were tectonically thickened (Fig. 11a & b).

In model 2, which simulated syn-diapiric shortening, a 1.3 cm thick viscous layer of SGM36 was buried under a 2 mm thick pre-kinematic overburden of loose sand. The model was shortened at a constant rate of 1.8 cm h^{-1} (5×10^{-3} mm s^{-1}). A 2 mm thick layer of loose sand was scraped over the top of the model every 6 min giving a bulk deposition rate of 1.8 cm h^{-1} (5×10^{-3} mm s^{-1}), which is the same as the shortening rate. Here, a salt swell formed as the model was shortened. The syn-kinematic layers onlaped the rising structure suggesting the presence of a bulge during their deposition (Fig. 11c & d). The thickness increase of the overburden units away from the bulge initiated a differential loading which drove the bulge up (Fig. 11c & d). However, this differential loading was overcome by the lateral stress applied due to the shortening. The bulge was then squeezed to a mullion cusp (Fig. 11c & d). Although shortening cannot thicken the overburden units as fast as the previous model, shortening squeezed the rising bulge to a mullion casp which thinned upwards and never became diapiric.

In model 3, which simulated post-diapiric shortening, a 2 cm thick layer of SGM36 was buried by 1 cm thick pre-kinematic layer of loose sand. An initial differential loading initiated several diapirs which were down-built by accumulating sand on their flanks. The model was then shortened by 10% from one end (at a rate of 3×10^{-3} mm s^{-1}). Most of the post-diapiric shortening was taken up by the 'softer' material in the stems of pre-existing diapirs. These were squeezed and closed resulting in a cut-off of the feeding stem of the pre-existing diapirs (Fig. 11e & f). The squeezed material moved upwards resulting in a temporarily increase in the elevation of the dynamic bulge (Fig. 11e & f).

DISCUSSION

Sediment accumulation (−erosion), salt supply (−dissolution) and extension (− shortening) mould salt diapirs. These parameters can be active simultaneously or at different times during the evolution of a diapir. In the previous sections it has been argued that the conventionally accepted plots of rate of sediment accumulation vs rate of salt supply can only represent the moulding history of a salt diapir in special cases (absence of E', Sh', Er' and D'). Lateral movement (extension and shortening) has a significant role in controlling the geometry of salt diapirs. For example, columnar diapirs could be the result of not only equal rates of sediment accumulation and salt supply, but also different combinations of rates of extension, sediment accumulation and salt supply (Fig. 2). It is argued here that it is not the rate of salt supply vs the rate of sediment accumulation which governs the geometry of salt diapirs. Instead, the rate of salt supply (S') vs the rate of extension multiplied by sediment accumulation $(E \cdot A)'$ is critical in controlling diapir geometry.

Pre-diapiric extension is a significant parameter in triggering diapirism (Vendeville and Jackson, 1992a). However, for syn-diapiric extension, it is not only the

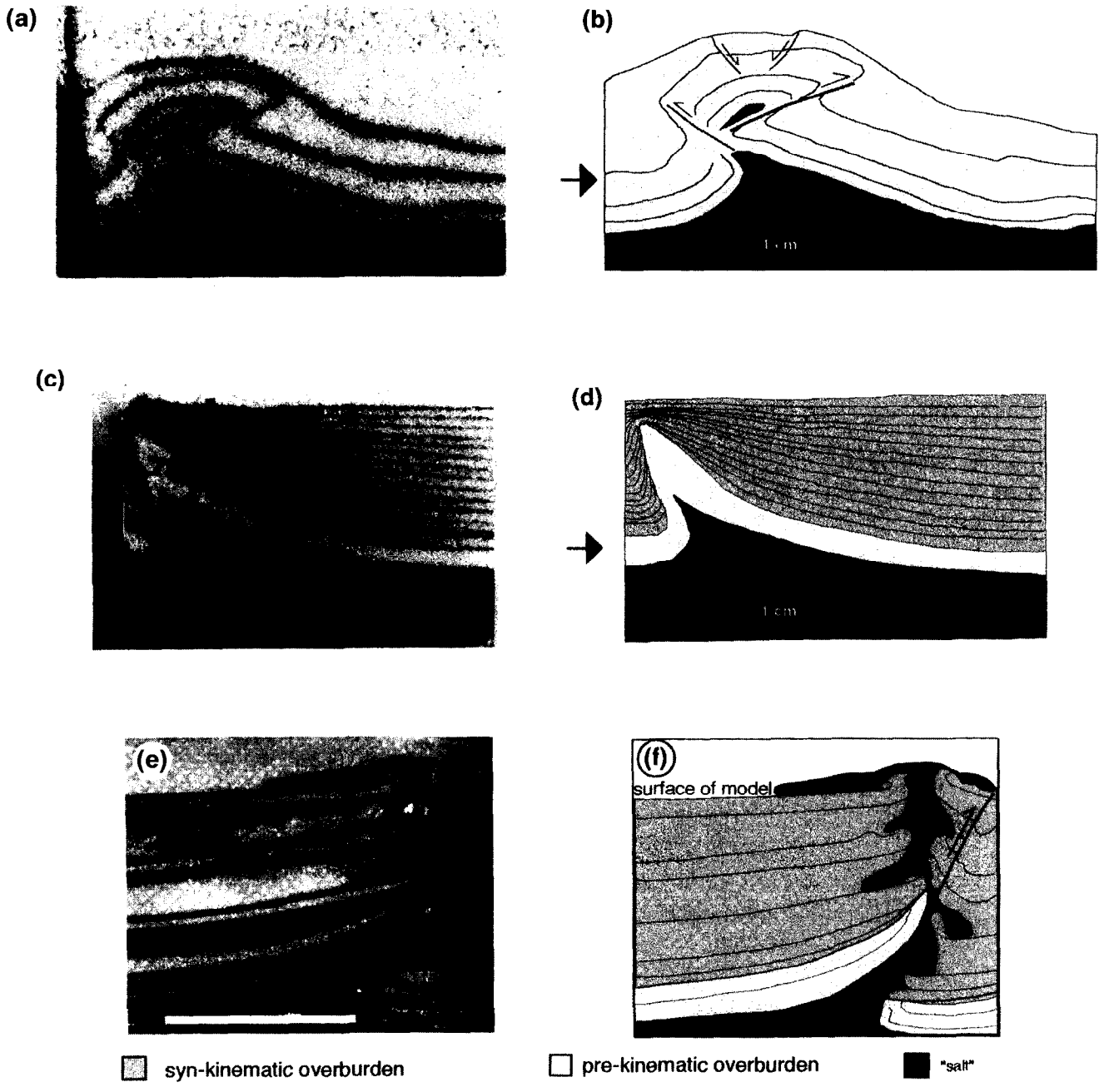

Fig. 11. (a) Photograph and (b) line drawing of a profile of an analogue model (model 1) showing the effect of pre-diapiric shortening on diapirism. During the shortening both the ductile layer and its overburden were tectonically thickened. The ductile layer accumulated in the core of the anticline in the overburden, which isolates a salt swell from its feeding stem. In nature the uplifted crest of the anticline, whose crest is collapsing above the ductile material in its core, if eroded gives the ductile material a chance to intrude. (c) Photograph and (d) line drawing of a profile of an analogue model (model 2) showing the effect of syn-diapiric shortening on diapirism. The ductile layer is mullioned beneath the folded overburden units. Overburden units onlap the structure indicating that the cusp was a topographic high during their deposition. (e) Photograph and (f) line drawing of a profile of an analogue model showing the effect of post-diapiric shortening on a pre-existing diapir. The diapir stem acts as a stress concentration zone during the shortening where the thrust initiates and pinches the feeding stem. The bar in (e) is 5 cm.

extension rate alone but the rate of the product of sediment accumulation multiplied by extension which governs the triggering mechanism and moulding of diapirs. By analysing the Lin (1992) models it can be shown here that even when extension rate is twice as large as the rate of sediment accumulation (experiment 39), only salt rollers form beneath the rapidly accumulating overburden units. In this case, extensional faults cut the rapidly accumulating overburden units into blocks that rotate along growth faults (Fig. 9a). In experiment 47, extension rate, which is 7 times greater than the rate of sediment accumulation, is still not fast enough to outpace the rate of sediment accumulation and assist the reactive diapir to grow actively (Fig. 9b).

In experiment 60, where the extension rate is more than one order of magnitude greater than the rate of sediment accumulation, several diapirs grow from the reactive stage to actively piercing their overburden and to passively grow at later stages (Fig. 9c). Experiment 60 is used in this study to comment in detail on the effect of rates of sediment accumulation, salt supply and extension on moulding salt diapirs.

Vendeville and Jackson (1991) and Lin (1992) used analogue models to discuss the influence of extension rate on the geometry of resulting diapirs in general. Here, the restored sections from experiment 60 of Lin (1992) are used to quantify the rates of salt supply, sediment accumulation and extension in order to illustrate the significance of each of these rates on the geometry of diapirs. From the model sections the rates of salt supply and diapir rise were calculated for three of the diapirs (G6, G9 and G10) (Figs 9c & 12). The rate of salt supply was calculated by measuring the diapir area at different times in each profile (Fig. 12a). The rate of diapir rise (Fig. 12b) was calculated by measuring the elevation of their crest above the upper boundary of the source layer with time. In experiment 60, the bulk rates of sediment accumulation and extension are 3.4×10^{-4} mm s^{-1} and 2.9×10^{-3} mm s^{-1}, respectively. These two rates are assumed to be constant for all the three diapirs used in this study. Limitation of this assumption is described later. Diapir G6, whose crest increases in elevation indicating vertical growth even at later stages of model deformation, possesses an upward-narrowing geometry even when its rise rate (5×10^{-4}–8.6×10^{-4} mm s^{-1}) (and even rate of salt supply 1.8×10^{-2} 2.5×10^{-2} mm^2 s^{-1}) is higher than the rate of sediment accumulation (3.4×10^{-4} mm s^{-1}). Conventionally, when rising rate is greater than the rate of sediment accumulation, an upward-widening diapir is expected to form. However, because diapir G6 (Fig. 9c) is simultaneously extended, the rate of rise cannot pace both the rates of extension and sediment accumulation. Here, extension counteracts the rate of salt supply by widening the space which the diapir needs to fill. Therefore, the diapir, which does not possess enough salt supply, narrows upward.

Rate of sediment accumulation multiplied by extension

As the amount of salt fed into a diapir is decisive in filling the space created by the extension and sediment accumulation, here salt supply is used instead of diapir rise as a significant parameter in moulding the geometry of the structure. The rate of salt supply (S') is compared to a new rate; the rate of sediment accumulation multiplied by extension ($E \cdot A)'$. This rate is calculated by measuring the amount of sediment accumulation (A) at a given time and multiplying it by the amount of extension (E) that took place during the same time interval. When extension is zero, this rate is represented only by the rate of sediment accumulation. The multiplication product is plotted against time for diapir G6 in experiment 60 (Fig. 9c) and the rate of sediment accumulation multiplied by extension is deduced from the plot (Fig. 13a). The amount of sediment accumulation multiplied by extension at a given time defines a rectangle whose width is the amount of extension and its height is the amount of sediment accumulation (Fig. 14). When the amount of salt supply (S) at a given time is equal to the area of the rectangle defined by sediment accumulation multiplied by extension, a columnar diapir forms (Fig. 14a). When the amount of salt supply at a given time is less than the area of the rectangle an upward-narrowing diapir forms (Fig. 14b). Whereas when the amount of salt supply at a given time is more than the area of the rectangle an upward-widening diapir forms (Fig. 14c). This two-dimensional approach can be converted to three dimensions by considering the volume of salt supply and comparing it to the volume of the cube whose width is the amount of extension, its height is the amount of sediment accumulation and its length is the extent of the diapir in three dimensions.

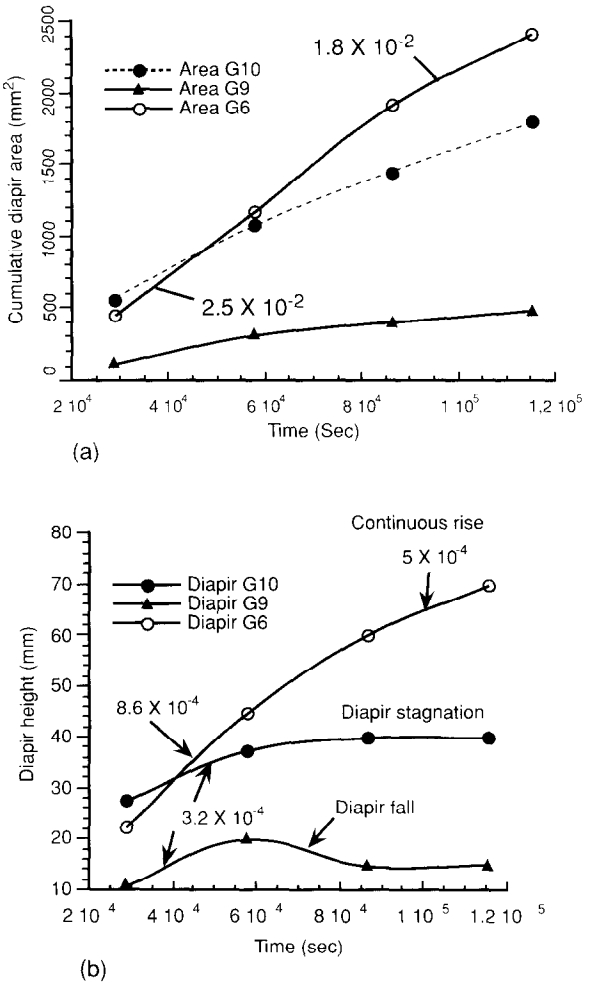

Fig. 12. Plots of (a) cumulative diapir area vs time and (b) diapir height with time for diapirs (G6, G9 and G10) in experiment 60 (see Fig. 10). The numbers outline the rate of salt supply (in a) and rate of diapir rise (in b) for the diapirs at corresponding time intervals.

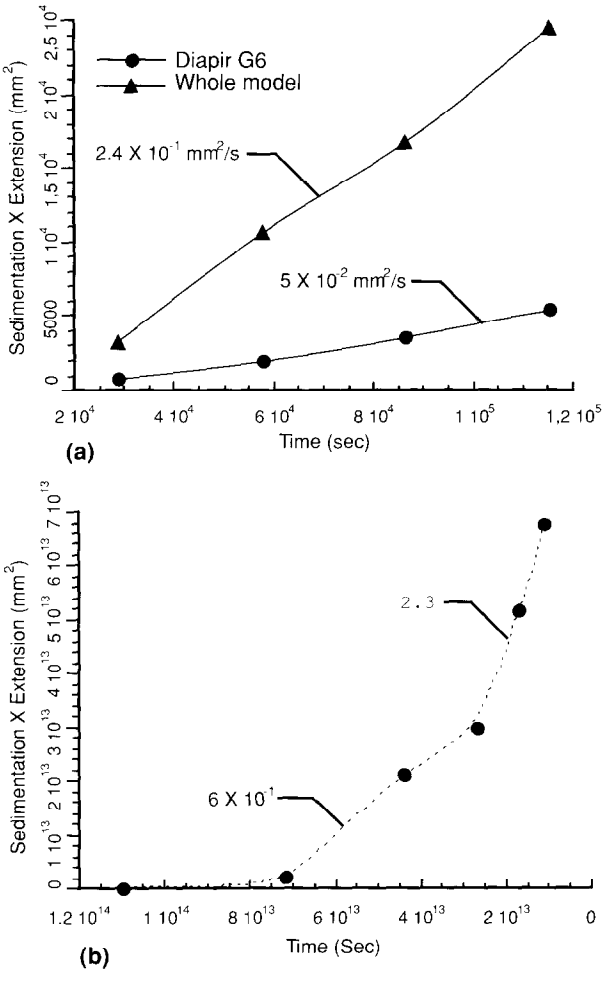

Fig. 13. (a) Plot of sediment accumulation multiplied by extension with time for the entire model and for one of the diapirs (G6) in experiment 60. Note that the bulk rate of sediment accumulation multiplied by extension is ≈ 5 times greater than the same rate for diapir G6. (b) A similar plot of sedimentation multiplied by extension with time for a depth-converted seismic profile from the eastern Green Canyon–Ewing Bank area of offshore Louisiana (after Rowan, 1993). Note that the rate of sediment accumulation multiplied by extension increases with time.

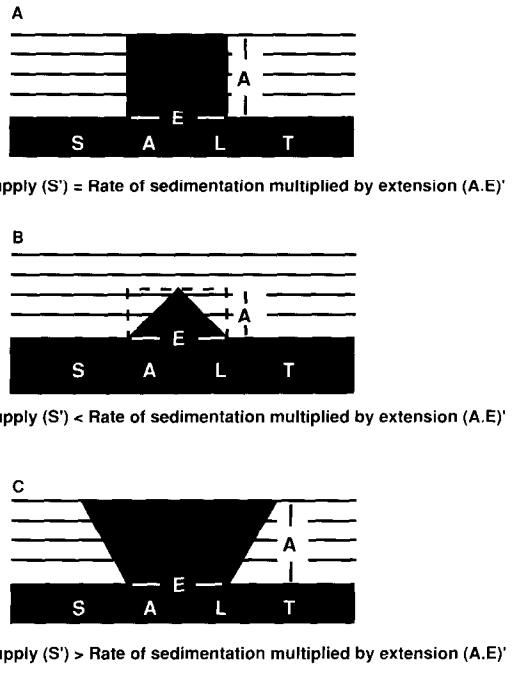

Fig. 14. Schematic illustration of relationship between the amount of salt supply and the rectangle defined by the amount of sediment accumulation multiplied by extension. A is the amount of sediment accumulation and E is the amount of extension. When the amount of salt supply is equal to the area of the rectangle, columnar diapirs form (a), when it is smaller, upward-narrowing diapirs form (b) and when it is greater, upward-widening diapirs form (c).

Following the arguments described above, diapirs in extensional areas can build upward-widening geometries when their rate of salt supply is greater than the bulk rate of sediment accumulation multiplied by extension. In experiment 60, the bulk rate of sediment accumulation multiplied by extension is equal to 2.4×10^{-1} mm^2 s^{-1} (Fig. 13a), which is one order of magnitude greater than the rate of salt supply (2.5×10^{-2} mm^2 s^{-1}) (Fig. 12a) for diapir G6, and 13–20 and 34–88 times higher than the rates of salt supply for diapirs G10 and G9, respectively (Fig. 12a). Therefore, all the three diapirs possess an upward-narrowing geometry.

In the above calculations, the bulk rates of salt supply, extension and sediment accumulation are used. However, even if the incremental rates are used, the above argument still holds for moulding the geometry of salt diapirs. To illustrate this point local extension rate was measured for two diapirs (G6 and G10 in Fig. 9c) in the restored profiles of experiment 60 and compared with the bulk extension rate (Fig. 15b). Figure 15 shows the incremental rate of salt supply and the rate of extension for diapirs G6 and G10 in experiment 60. The bulk extension rate is up to 7 times higher than the local extension rate at the base of diapir G6 and G10 (Fig. 15b). The *incremental* rate of sediment accumulation multiplied by extension (5×10^{-2} mm^2 s^{-1}) is 5 times smaller than the *bulk* rate of sediment accumulation multiplied by extension (2.4×10^{-1} mm^2 s^{-1}) (Fig. 13a), but it is still 5 times greater than the incremental rate of salt supply (9.1×10^{-3} mm^2 s^{-1}) of diapir G6 and 12 times greater than the incremental rate of salt supply (4×10^{-3} mm^2 s^{-1}) for diapirs G9 (Fig. 15a). Therefore, the diapirs narrow upwards during their evolution. It is worth mentioning that the incremental rather than bulk rates are more appropriate to use for backward moulding of diapirs because diapirs are moulded incrementally with time.

In general, when the rate of salt supply cannot keep up with both filling the additional lateral space created by the extension and the vertical space created by the accumulating sediments, the diapir narrows upwards (Fig. 14b). Only if the rate of salt supply is greater than the rate of sediment accumulation multiplied by extension can a salt diapir possess an upward-widening geometry (Fig. 14c). On the other hand, when the rate of salt supply is equal to the rate of sediment accumulation multiplied by extension, columnar diapirs form (Figs 2 & 14a).

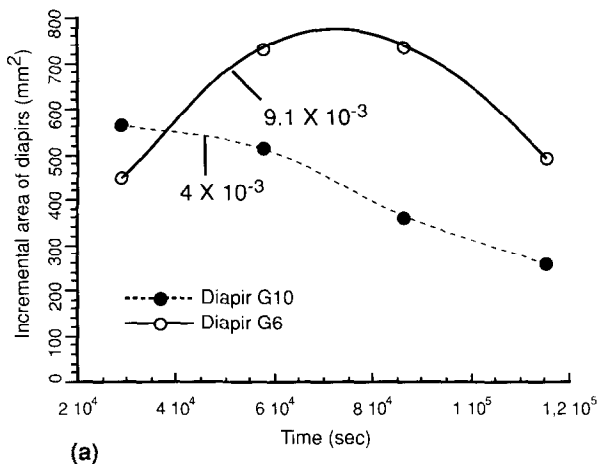

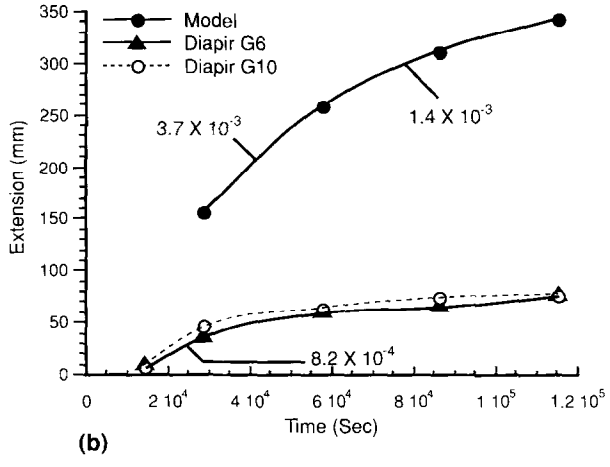

Fig. 15. Plots of (a) incremental area of diapirs G6 and G10 with time in experiment 60. (b) bulk and local extension with time in experiment 60.

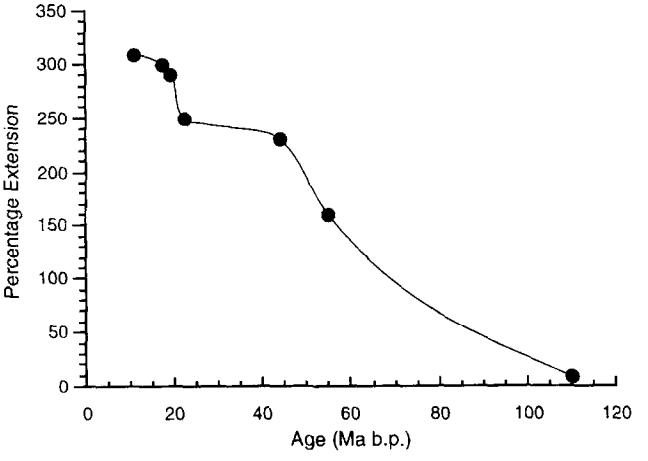

Fig. 16. Extension through time of the Quenguela Graben, Kwanza Basin. The plot is prepared from cross-sectional restoration by Duval *et al.* (1992). The curve shows that the Kwanza Basin has suffered two phases of extension.

Application to nature

When thin-skinned extension is a result of gravity gliding on a ductile substrate it can be assumed that extension decreases significantly as the thickness of the ductile detachment decreases. This decrease in the extension rate is documented both in the models described above and in natural examples. Duval *et al.* (1992, fig. 10) restored a cross-section of Quenguela graben, Kwanza Basin, to argue for 3.1 stretch (210% extension) during 99 Ma. Their restored profiles show a significant decrease in extension with time (Fig. 16), which can be attributed to the decrease in the thickness of salt layer at later stages of deformation. In the Kwanza Basin two main phases of extension occurred in 99 Ma (Duval *et al.*, 1992) suggesting that extension has not been continuous in time (Fig. 16). Extension rate in a sedimentary basin can be hetrogeneous in space as well. Even when the bulk extension rate is known, the amount of extension which individual diapirs are subjected to in a basin may vary significantly depending on the local variation in thickness of salt surrounding the diapirs and the location of the diapir in the basin. In other words, the extension rate which individual diapirs are subjected to could be different from the bulk extension rate in a sedimentary basin. In order to overcome this problem, the local extension rate instead of the bulk extension rate should be considered for backward mould diapirs. In fact, it is this local extension rather than the bulk extension rate which is significant for moulding the geometry of salt diapirs.

In nature, extension rate varies between 0.4 and 2 mm y^{-1} (examples: Kwanza Basin, Duval *et al.*, 1992; Ewing Bank, Rowan, 1993), whereas the rate of diapir rise based on structures in the well-explored Gulf of Mexico (Jackson and Talbot, 1991) and in the North Sea (Talbot, 1995) ranges between 0.01 and 2 mm y^{-1}. The rate of sediment accumulation on the other side is more variable depending on whether it is short- or long-term sediment accumulation. Short-term sediment accumulation could be a few tens of centimetres per day, whereas geologically determined rates (long-term), which are more relevant to this study, average out to a few millimetres per million years. Rowan (1993) sequentially restored an interpreted seismic profile from the eastern Green Canyon–Ewing Bank area of offshore Louisiana. He measured and calculated the net extension and sediment accumulation with time. From his data (Rowan, 1993, fig. 6) the rate of sediment accumulation times extension $(E \cdot A)'$ is calculated and is shown in Fig. 13(b). Any of the diapirs influenced by this extension and whose rate of salt supply is less than this rate, which increased four-fold in the last 2 Ma, would not be able to outpace it and therefore possess an upward-narrowing geometry. Indeed, the diapirs shown in the depth section from Rowan (1993) possess an upward-narrowing geometry. Therefore, it could be suggested that, in general, in extensional basins (and passive margins) the rate of sediment accumulation and extension outpace the rate of salt supply. Following this line of argument, the lack of

upward-widening and columnar diapirs in passive margins (e.g. Kwanza Basin and Santos Basin) suggest that the rate of salt supply was lower than the rate of extension multiplied by sediment accumulation during the formation of the diapirs. The Gulf of Mexico is different because there a fast aggradation rate has driven the Louann salt down-dip to form asymmetric salt diapirs, with broad overhangs spreading down-dip.

This argument could be taken one step further by suggesting that the presence of columnar and upward-widening salt diapirs in any basin suggest an insignificant extension during the evolution of the structures. Unlike sediment accumulation and extension, salt supply to any salt diapir is limited and ceases eventually with time when the feeding source layer depletes or is cut-off. This means that when a salt layer is divided into separate salt rollers by fault-bounded overburden blocks during rapid extension at the beginning of deformation in a basin, it would not be able to supply any of the structures even when extension ceases totally at later stages.

Shortening folds and/or thrusts overburden units above a salt décollement. Mullions and cusps (Talbot *et al.*, 1988) may form at the overburden–salt interface. Unlike extension, shortening thickens overburden units tectonically and discourages piercement. It is more difficult for diapirs to overcome the increased strength of the thickened overburden units. In other words, shortening increases the rate of 'sediment accumulation'. Pre-diapiric shortening suppresses diapirism by vertically increasing the thickness of their overburdens before any diapirs get the chance to form. Syn-diapiric shortening suppresses diapirism by laterally squeezing any rising domes and tectonically thickening their overburden. Therefore, syn-diapiric shortening moulds cusp-like diapirs which are squeezed laterally and are prevented from growing. On the other hand, post-diapiric shortening may cut the feeding stem and 'kill' a pre-existing diapir. Shortening squeezes salt in a diapir stem and thus contributes to an increase in salt supply (Vendeville and Nilsen, 1995). But this increase in salt supply is temporary and decreases sharply when shortening closes and empties the feeding stem of the diapir. During shortening diapirs act as stress concentration zones where folds/thrusts may form and propagate (Koyi, 1988). Thrusts propagate further and cut the feeding stem of the diapir (Fig. 11e & f). In nature, these diapirs would sag with time. Some of the inactive diapirs in the Zagros mountain belt (Talbot and Alavi, 1996) may have their feeding stems cut-off during the Zagros orogeny. These diapirs form large dissolution craters on the surface as the salt in their dynamic bulge dissolves.

CONCLUSIONS

The geometry of salt diapirs may be the result of different combinations of six parameters: namely the rates of sediment accumulation (A'); salt supply (S'); extension (E'); erosion (Er'); dissolution (D'); and shortening (Sh') at different times.

Extension influences the geometry of salt diapirs by increasing the lateral space they occupy and it aids salt movement as long as salt supply is not depleted.

Compression thickens overburden units, increases its strength and laterally squeezes the feeding stem of any existing diapir. Consequently, it impedes diapirism.

This study introduces a new rate of the product of extension multiplied by sediment accumulation and allows reinterpretation of conventionally classified upward-narrowing, upward-widening and columnar diapirs. Upward-narrowing diapirs form when the rate of salt supply is less than the rate of sediment accumulation multiplied by extension rate. Upward-widening diapirs form when the salt supply is greater than the rate of sediment accumulation multiplied by extension rate. Columnar diapirs form when the rate of salt supply is equal to the rate of sediment accumulation multiplied by extension rate. This new classification illustrates the significance of extension in moulding the geometry of salt diapirs.

This study suggests that due to a high rate of extension (and probably rate of sediment accumulation) in passive margins, the rate of salt supply cannot support columnar or upward-widening diapirs. In these areas salt rollers or upward-narrowing diapirs are more likely to form.

Acknowledgements—Thanks are due to Ian Alsop, Mike Hudec, Christopher Talbot and Bruno Vendeville for commenting on an earlier version of this manuscript. Lyal Harris and James Cotton are thanked for commenting on the revised version of the manuscript. Review comments by Gijs Remmlets, Cees Passchier and an anonymous reviewer are greatly appreciated. This work is funded by the Swedish Natural Science Research Council (NFR).

REFERENCES

Barton, D. C. (1933) Mechanics and formation of salt domes with special reference to Gulf coast domes of Texas and Louisiana. *Bulletin of the American Association of Petroleum Geologists* **17**, 1025–1083.

Duval, B., Cramez, C. and Jackson, M. P. A. (1992) Raft tectonics in the Kwanza Basin, Angola. *Marine and Petroleum Geology* **9**, 389–404.

Jackson, M. P. A. and Talbot, C. J. (1989) Anatomy of mushroom-shaped diapirs. *Journal of Structural Geology* **11**, 211–230.

Jackson, M. P. A., Cornelius, R. R., Gansser, A., Stocklin, J. and Talbot, C. J. (1990) *Salt Diapirs of the Great Kavir, Central Iran.* Geological Society of America Memoir **177**.

Jackson, M. P. A. and Talbot, C. J. (1991) *A Glossary of Salt Tectonics.* Bureau of Economic Geology, University of Texas at Austin, Geological Circular **91-4**.

Jackson, M. P. A., Vendeville, B. C. and Schultz-Ela, D. D. (1994) Structural dynamics of salt systems. *Annual Review of Earth and Planetary Sciences* **22**, 93–117.

Koyi, H., Talbot, C. J. and Tørudbakken, B. O. (1993) Salt diapirs of the southwestern Nordkapp Basin: analogue modelling. *Tectonophysics* **228**, 167–187.

Koyi, H. (1988) Experimental modeling of role of gravity and lateral shortening in Zagros mountain belt. *AAPG Bulletin* **72**, 1381–1394.

Lin, H. T. (1992) Experimental study of syndepositional and postdepositional gravity spreading of a brittle overburden and viscous substratum. M.Sc. thesis, Department of Geological Sciences, University of Texas at Austin.

McGuinness, D. B. and Hossack, J. R. (1993) The development of allochthonous salt sheets as controlled by the rates of extension, sediment accumulation, and salt supply. In *Fourteenth Annual Research Conference, Gulf Coast Section*, pp. 127–149. SEPM Foundation, Houston, Texas.

Nalpas, T. and Brun, J. P. (1993) Salt flow and diapirism related to extension at crustal scale. *Tectonophysics* **228**, 349–362.

Nelson, T. H. (1991) Salt tectonics and listric normal faults. In *The Gulf of Mexico Basin*, ed. A. Salvador, pp. 73–89. Geological Society of America, The Geology of North America **J**.

Nyland, B., Jensen, L. N., Skagen, J., Skarpnes, O. and Vorren, T. (1992) Tertiary uplift and erosion in the Barents Sea; magnitude, timing and consequences. In *Structural and Tectonic Modelling and its Application to Petroleum Geology*, eds R. M. Larsen, H. Brekke, B. T. Larsen and E. Talleraas, pp. 153–162. Norwegian Petroleum Society (NPF) Special Publication **1**.

Ramberg, H. (1967) *Gravity, Deformation and the Earth's Crust*, 1st edn. Academic Press, New York.

Riis, F. and Fjeldskaar, W. (1992) On the magnitude of late Tertiary and Quaternary erosion and its significance for the uplift of Scandinavia and the Barents Sea. In: *Structural and Tectonic Modeling and its Application to Petroleum Geology*, eds Larsen *et al.* Norwegian Petroleum Society Special Publication, 163–185.

Rowan, M. G. (1993) A systematic technique for sequential restoration of salt structures. *Tectonophysics* **228**, 331–348.

Richardsen, G., Vorren, T. O. and Tørudbakken, O. B. (1993) Post-Early Cretaceous uplift and erosion in the southern Barents Sea: a discussion based on analysis of seismic interval velocities. *Norsk Geologisk Tidsskrift* **7**, 3–22.

Schmeling, H. (1987) On the relation between initial conditions and late stages of Rayleigh–Taylor instabilities. *Tectonophysics* **133**, 16–31.

Seni, S. J. and Jackson, M. P. A. (1983) Evolution of salt structures, east Texas diapir province, part 2: Patterns and rates of halokinesis. *Bulletin of the American Association of Petroleum Geologists* **67**, 1245–1274.

Talbot, C. J. (1995) Moulding of salt diapirs by stiff overburden. In *Salt Tectonics: A Global Prospective for Exploration*, eds M. P. A. Jackson, R. G. Roberts and S. Snelsen. American Association of Petroleum Geologists Memoir. 65 pp.

Talbot, C. J. and Alavi, M. (1996) The past of a future syntaxis across the Zagros. In *Salt Tectonics* eds G. I. Alsop, D. J. Blundel and I. Davison, pp. 89–109. Geological Society of London Special Publication **100**.

Talbot, C. J., Koyi, H., Mulugeta, G. and Sokoutis, D. (1988) Identification of evaporite diapirs formed under the influence of horizontal compression. *Bulletin of Canadian Petroleum Geology* **36**, 91–95.

Trusheim, F. (1960) Mechanism of salt migration in northern Germany. *AAPG Bulletin* **44**, 1519–1540.

Vendeville, B. C. and Jackson, M. P. A. (1991) Deposition, extension and the shape of down-building salt diapirs (Abstract). *Bulletin of the American Association of Petroleum Geologists* **75**, 687–689.

Vendeville, B. C. and Jackson, M. P. A. (1992a) The rise of diapirs during thin-skinned extension. *Marine and Petroleum Geology* **9**, 331–353.

Vendeville, B. C. and Jackson, M. P. A. (1992b) The fall of diapirs during thin-skinned extension. *Marine and Petroleum Geology* **9**, 354–371.

Vendeville, B. C. and Nilsen, K. (1995) Episodic growth of salt diapirs driven by horizontal shortening. In *Proceedings of Sixteenth Annual Research Conference, Gulf Coast Section*, pp. 285–295. SEPM Foundation, Houston, Texas.

Whitehead, J. A. and Luther, D. S. (1975) dynamics of laboratory diapirs and plume models. *Journal of Geophysical Research* **80**, 705–717.

Woidt, W. D. (1980) Finite element calculations applied to salt dome analysis. *Tectonophysics* **50**, 369–386.